frontiers | Frontiers in Water

TYPE Original Research
PUBLISHED 18 September 2024
DOI 10.3389/frwa.2024.1447577

OPEN ACCESS

EDITED BY
George P. Karatzas,
Technical University of Crete, Greece

REVIEWED BY
Kristian Förster,
Weihenstephan-Triesdorf University of Applied Sciences, Germany
Antonio Annis,
University of Padua, Italy

*CORRESPONDENCE
Assane Ndiaye
✉ ndiaye.assane@edu.wascal.org;
✉ assanendiaye58@gmail.com

RECEIVED 11 June 2024
ACCEPTED 04 September 2024
PUBLISHED 18 September 2024

CITATION
Ndiaye A, Arnault J, Mbaye ML, Sy S, Camara M, Lawin AE and Kunstmann H (2024) Potential contribution of land cover change on flood events in the Senegal River basin.
Front. Water 6:1447577.
doi: 10.3389/frwa.2024.1447577

Potential contribution of land cover change on flood events in the Senegal River basin

Assane Ndiaye[1,2]*, Joël Arnault[3,4], Mamadou Lamine Mbaye[5], Souleymane Sy[4], Moctar Camara[5], Agnidé Emmanuel Lawin[1,2] and Harald Kunstmann[3,4,6]

[1]Graduate Research Program on Climate Change and Water Resources, West African Science Service Center on Climate Change and Adapted Land Use (WASCAL), University of Abomey-Calavi, Abomey-Calavi, Benin, [2]Laboratory of Applied Hydrology, University of Abomey-Calavi, Abomey-Calavi, Benin, [3]Karlsruhe Institute of Technology, Institute of Meteorology and Climate Research (IMK) IFU, Garmisch-Partenkirchen, Germany, [4]Institute of Geography, University of Augsburg, Augsburg, Germany, [5]Laboratoire d'Océanographie, des Sciences de l'Environnement et du Climat (LOSEC), Université Assane SECK de Ziguinchor, Ziguinchor, Senegal, [6]Centre for Climate Resilience, University of Augsburg, Augsburg, Germany

The increase in flood events observed in West African countries, and often in specific river basins, can be influenced by several factors, including anthropogenic land use and land-cover changes. However, the potential contribution of land cover changes to flood events still needs to be explored, especially in West Africa. Here, the fully coupled atmosphere-hydrology WRF-Hydro system, which comprises an atmospheric model and additionally incorporates the surface, subsurface, overland flow, and channel routing, is used to investigate the potential impact of a land cover change scenario on flood events in the Senegal River basin. The simulation was performed from 2010 to 2020, with a calibration period spanning from 2011 to 2012 and a validation period from 2013 to 2020. Several skill scores, including Nash-Sutcliffe Efficiency (NSE), BIAS, and Kling-Gupta Efficiency (KGE), were utilized to assess the calibration and validation performances. Additionally, two planetary boundary layer schemes (PBL5 and PBL7) were used to determine their associated uncertainty. Our results show that the best calibration results (NSE = 0.70; KGE = 0.83; PBIAS = −7% and BE = 0.67) in the Senegal River basin are obtained with PBL5 when the calibration is performed with a SLOPE parameter 0.03. A similar good performance was also obtained for the validation with NSE = 0.74, KGE = 0.84, and PBIAS = −8%. Likewise, our findings indicate that converting savanna to woody savannas can elevate water resources, with a 2% rise in precipitation and a 4% increase in runoff. This transition also correlates with an increase in moderate flood events (3500–4000 m^3/s), a decrease in severe floods (4000–5000 m^3/s), and their associated occurrence of extreme floods (>5000 m^3/s) in the Senegal River basin.

KEYWORDS

land cover change, WRF-Hydro, Senegal River basin, overbank flow, flood events

1 Introduction

Climate hazards manifest differently from one locality to another. At both global and local scales, increased flood risks have been noted due to climate change and other processes such as urban expansion and anthropogenically land use and land-cover changes (Kundzewicz et al., 2014; Kadri and Kurniyaningrum, 2019; Prăvălie et al., 2019; Costache et al., 2019; Babaei et al., 2018). The frequency of significant floods appears to be increasing worldwide (Hall et al., 2014; Najibi and Devineni, 2018; Hirabayashi et al., 2021), particularly in developing countries such as West Africa, where populations remain vulnerable to extreme climates and their associated flooding events. These events have become more frequent (Déqué et al., 2017; Cardona et al., 2012).

In West Africa, however, the spatial distribution of these extreme events is not homogeneous (Ta et al., 2016). In Côte d'Ivoire, the observed increase in heavy precipitation over the past 15 years (Konate et al., 2023), has increased flooding, particularly in urban areas where authorities and residents are not adequately prepared, exposing infrastructure and human safety to heightened risks. In Niger, annual flooding episodes have been recorded in the coastal states of the Niger Delta, located along the Niger River and its tributaries (Mmom and Aifesehi, 2013).

In Mali, an analysis of the flood report showed an increase in the intensity and frequency of extreme precipitation in Bamako from 1982 to 2019 (Fofana et al., 2022). Burkina Faso experienced approximately three floods per year from 1986 to 2016 according to Tazen et al. (2019). In Senegal, heavy rainfall frequently leads to flooding, particularly impacting low-lying urban areas (Young et al., 2019). Between 1980 and 2009, floods in Senegal affected over 900,000 people, resulting in 45 deaths and causing material damages estimated at over 142 million US dollars, according to the Ministry of Environment and Sustainable Development in 2015 (Zermoglio et al., 2015). In the Senegal River basin, Ndiaye et al. (2023) highlighted an increase in the number of flood occurrences in recent years.

However, several factors, such as changes in land use land cover, can influence these increases in floods observed in West African countries and often in specific basins (Rogger et al., 2017). Several studies have been conducted to assess the impact of land use change (deforestation/afforestation) on rainfall extreme weather indices in West Africa (Camara et al., 2022; Sy and Quesada, 2020; Abiodun et al., 2013). Focusing on the effects of reforestation on the Sahel-Saharan interface on extreme events in the Sahel region during the West African monsoon season, using the RegCM4 model, Camara et al. (2022) showed an increase in the number of wet days (R1mm) in both above and outside the reforested area. Investigating the consequences of afforestation on future extreme weather events in Nigeria, Abiodun et al. (2013) demonstrated that afforestation can also increase the frequency of extreme rainfall events and increase the flood events in the coastal region.

Nevertheless, the potential contribution of land use changes to flood events remains unexplored, especially in the Senegal River Basin located between four West African countries - Senegal, Mali, Mauritania, and Guinea. Few studies have investigated the land use change in the Senegal River basin. For instance, Astou Sambou et al. (2023) using the Landsat images from 1986, 2006, and 2020, along with the Random Forest classification method, investigated the past and future evolution of change of land use in the watersheds of the Bafing and Falémé rivers, which are tributaries located in the Senegal River Basin. Their findings indicate that from 1986 to 2020, Bafing witnessed a notable rise in vegetation, water, agricultural zones, and settlements, accompanied by a decline in bare ground. Projections for 2050 indicate a further increase in vegetation, agricultural areas, and settlements, suggesting an environmental impact. Faty et al. (2019) investigate the impact of the land use dynamics in the context of hydrological regime variations in the upper basin of the Senegal River. Their aim was to assess the climatic vulnerability of water resources in the Senegal and Gambia River basins. They employed historical data on annual rainfall and streamflows from various tributaries, including Bafing Makana station, Senegal; Bakel station, Bakoye, Oulia; and Faleme at Kidira, spanning from 1955 to 2014. Additionally, they utilized Modis-Terra satellite images from 2007 and 2014. They showed throughout the study area, precipitation patterns underwent significant changes, with a westward shift of high precipitation isohyets. This resulted in an overall decrease in annual precipitation, an increase in average annual temperatures and sunshine, and a reduction in the duration of the rainy season.

Numerous studies have also attempted to analyze the impact of land use change on flooding events using satellites and Random Forest approaches (Acuña-Alonso et al., 2022; Thapa and Prasai, 2022; Banjara et al., 2024). However, it is worth noting that this approach fails to sufficiently capture the large-scale and non-local atmospheric responses triggered by land-use change (Sy et al., 2017). Neglecting these influences may result in an incomplete evaluation of the full effects of land cover on extreme floods at the river basin scale.

To our knowledge, no study has investigated the impact of land cover change on flood events using the fully coupled atmospheric-hydrological model (WRF-Hydro) system (Gochis et al., 2020). Here, for the first time, utilizing a coupled atmospheric-hydrological modeling system (WRF-Hydro), which incorporates the surface, subsurface, overland flow, overbank flow and channel routing (Arnault et al., 2023), this study aims to evaluate whether land-based mitigation policies, such as converting savannah to woody savannas in the upper Senegal River Basin, would have a significant impact on flood events. In other words, the paper aims to investigate the critical aspect of understanding the potential flood risks related to land cover change.

The remainder of this article is structured as follows. Section 2 describes the study area, datasets used for model calibration and validation, the WRF-Hydro model setup, and configuration, as well as the land use change realized experiments. The discussion of the most relevant results is provided in Section 3, while the summary and conclusion are provided in Section 4.

2 Materials and methods

2.1 Study area and observational datasets

The Senegal River basin (see Figure 1), located in West Africa, extends between 10° North latitude in Guinea and 17° North latitude in Mauritania. In longitude, the basin ranges from 7° west to 16° west. It covers an area of 300,000 km^2 and spans a length of 1800 km (Faye et al., 2015).

The basin is fed by three tributaries: the Falémé, the Bakoye, and the Bafing, originating from the high plateaus of the Fouta Djallon in

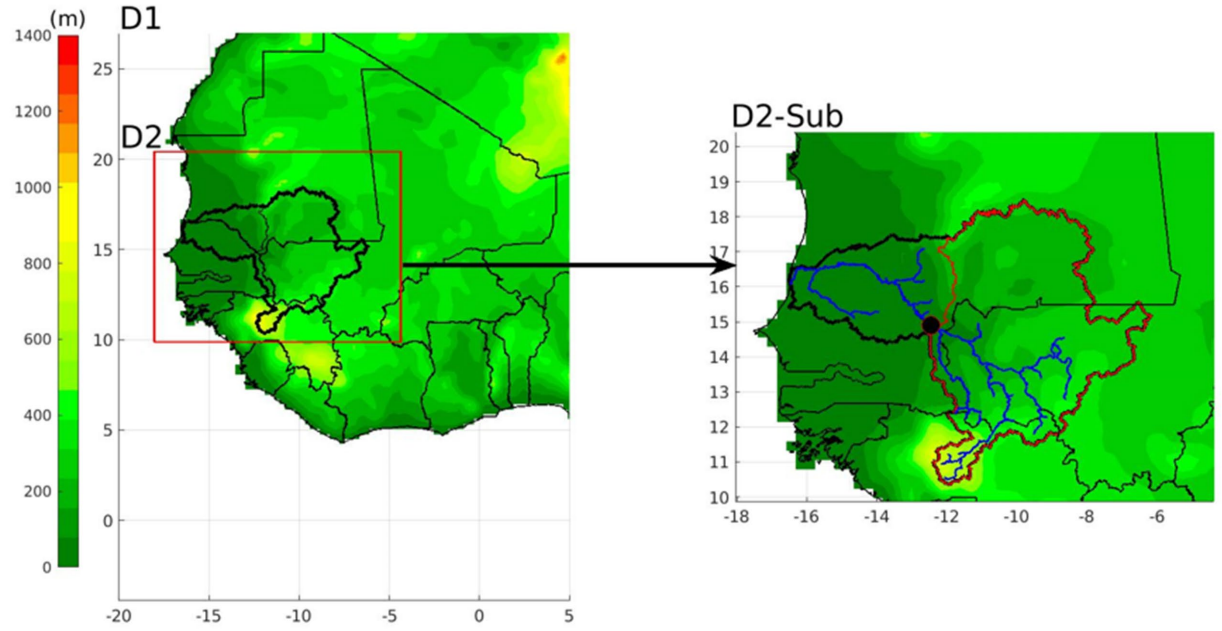

FIGURE 1
Topography (in meters above sea level) of the outer and inner domains, D1 and D2, at 30 km and 10 km resolution, respectively. The sub-domain, D2-sub, is represented at a resolution of 1 km, coupled with D2 for water routine computations. The red rectangle indicates the location of D2. The red contour line and blue curved line delineate the upper basin of the Senegal River, main rivers, and the outlet gage station (denoted by a black point) within D2-sub, referred to as the BAKEL station. The topography color scale provided by the color bar on the left side of D1 is consistent for both panels.

Guinea. The Bafing and Bakoye tributaries are located in Mali, as well as the Falémé, which borders Senegal and Mali and sometimes traverses Senegalese territory. The basin is divided into three main regions: the upper basin, the valley, and the delta. From a climatic perspective, the rainy season lasts for 4 months in Bakel, from June to September, and for 3 months, from July to September, in Matam, Podor, and Saint-Louis. The yearly average precipitation ranges from 500 to 1500 mm (Ndiaye et al., 2021). The streamflow at the Bakel reference station averaged 485 m3/s over the 40-year period, with a median of 254 m3/s and a standard deviation of 631 m3/s according Ndiaye et al. (2023). The vegetation in the region primarily follows a rainfall gradient, transitioning from semi-arid savannah in the North to sub-humid forest in the South (Stisen et al., 2008).

In this watershed, approximately 3.5 million people derive most of their income from middle resources, managed by the OMVS (Organization for the Development of the Senegal River).

The reference datasets to evaluate model performances are a gridded precipitation observation product and discharge data. The IMERG database (Integrated Multi-satellite Retrievals for Global Precipitation Measurement), developed by Huffman et al. (2014), is an almost global dataset, updated daily, presented on a regular grid with a horizontal resolution of 0.1°, and available for the period from 2001 to 2020. This product can be obtained by following the link.[1] Discharge data originates from the outlet (Bakel station), located at the exit of the upper basin (depicted by the red line), at coordinates (14.9°N, 12.4°W), as shown in Figure 1 (on the right). They were provided by the Directorate of Water Resources Management and Planning of Senegal (DGPRE) in the form of a daily time series covering the period from 2010 to 2020.

2.2 WRF-Hydro model setup

The WRF-Hydro model used for this study is the version of Arnault et al. (2023) enhanced with the description of overbank flow. It is built upon version 4.4 of the WRF climate model by Skamarock et al. (2021), coupled with version 5.2 of the WRF-Hydro hydrological module (Gochis et al., 2021). The model employs a sophisticated approach to represent atmospheric dynamics, using a three-dimensional grid that spans a specific geographical area. It incorporates a diverse range of parameterizations aimed at capturing the nuances of physical processes at a fine scale, covering aspects such as radiation, turbulence, cumulus convection, cloud microphysics, and terrestrial hydrology.

For our study, we define two nested modeling domains, as illustrated in Figure 1: a large external domain with a horizontal resolution of 30 km (121 × 121 grid points), encompassing the West Africa region, and a confined internal domain with a horizontal resolution of 10 km (151 × 121 grid points), centered on the Senegal River basin. The model domains include 50 vertical levels up to 10 hPa. The initial conditions and lateral boundaries of the external domain are tightly controlled, with atmospheric pressure, geopotential, zonal and meridional winds, temperature, and water vapor data sourced from ERA5 reanalysis (Hersbach et al., 2020). These data are provided at six-hour intervals, with a resolution of 0.25°. The internal domain is driven by the external domain through a one-way nesting

1 https://gpm.nasa.gov/data/directory

TABLE 1 Experimental details of the atmosphere model, WRF and WRF-Hydro.

WRF Physics options (D1 and D2)	Option	References
Projection resolution	Mercator	
Microphysics	WSM6	Hong and Lim (2006)
Cumulus parametrisation	Grell-Freitas	Grell and Freitas (2014)
Planetary boundary layer	MYNN2 ACN2	Nakanishi and Niino (2004) Pleim (2007)
Land surface model	Noah-MP	Niu et al. (2011)
Longwave radiation	RRTM	Mlawer et al. (1997)
Shortwave radiation	Dudhia	Dudhia (1989)
WRF-Hydro Physics options (D2)		
Subsurface routing (SUBRTSWCRT)	1, yes	Gochis et al. (2021)
Overland flow routing (OVRTSWCRT)	1, yes	
Channel routing (CHANRTSWCRT)	1, yes	
Baseflow bucket model (GWBASESWCRT)	0, no	
Overbankflow (OVERBANKFLOWSWCRT)	1, yes	Arnault et al. (2023)

method. Atmospheric motion equations in both domains are solved at time intervals of 80 s for the external domain and 40 s for the internal domain to ensure model stability. Both domains (D1 and D2) share the same physical parameterization for the WRF part (see Table 1). The choice of this parameterization is motivated by good values of scores [KGE (Gupta et al., 2009), NSE (Nash and Sutcliffe, 1970), and BIAS] of mean daily flows noted between observation and simulation during the calibration.

To evaluate model physics' uncertainty, two planetary boundary layer (PBL) schemes are used: PBL5 (Nakanishi and Niino, 2004) and PBL7 (Pleim, 2007). The choice of these PBL schemes is based on their specific characteristics, wet for PBL5 and dry for PBL7. Our choice of the two schemes PBL5 and PBL7 aims to determine the model uncertainty and also to observe its behavior under both wet and dry physical conditions.

Noah-MP, integrated into the WRF-Hydro setup used in this study, is a module dedicated to the land surface. It analyzes the evolution of vegetation cover and soil moisture in a column of 2 m depth, segmented into four distinct layers. The land use categories option "Moderate Resolution Imaging Spectroradiometer (MODIS)" land cover map (Friedl et al., 2002) is selected.

The WRF-Hydro routine modules are activated for the D2 domain through a coupling with the D2-sub subgrid with a resolution of 1 km. D2-sub is generated with the WRF-Hydro preprocessor tools and elevation data from the Hydrological and Topographic Database (HydroSHEDS) (Lehner et al., 2008). The Disaggregation between D2 and D2-sub is performed using a disaggregation factor. This factor is updated at the end of each time step after consideration of the routing processes calculated on D2-sub (Gochis et al., 2021). In this study, the base flow bucket model (GWBASESWCRT) is not used. As in Arnault et al. (2016), for a West African Sahelian watershed, no groundwater bucket option is retained because the base flow generated by this method would lead to higher water input into the river compared to observations (not shown).

2.3 Calibration and validation of WRF-Hydro coupled

A WRF-Hydro simulation is conducted over a period of 11 years, from 2010 to 2020, including a one-year spin up period. The WRF-Hydro model is calibrated for a 2-year period (2011–2012) and validated for the period from 2013 to 2020 in the Senegal River basin. Our calibration period is considered sufficiently long to obtain robust results with the WRF-Hydro model. The simulated discharge is calibrated by focusing on one sensitive parameter governing the amount of percolation (SLOPE), following the calibration strategy proposed in Arnault et al. (2023). Two other sensitive parameters: Manning's roughness coefficient for rivers (MannN), and the runoff infiltration partitioning parameter (REFKDT) are kept constant during our calibration process. The parameter sensitivity analysis we conducted is only partial, due to the limited amount of computing resources available.

Thus, our calibration is based on varying the SLOPE across different ranges (0.01, 0.03, 0.04, 0.06, 0.08), while the parameters REFKDT (3) and MannN (see Table 2) are set to default. These combinations are tested during the calibration based on planetary boundary layers PBL5 and PBL7 (see Table 2).

The calibration and validation discharge results are evaluated using skill scores such as percentage bias (Equation 1), Nash-Sutcliffe efficiency [NSE, Equation 2, (Nash and Sutcliffe, 1970)], Kling-Gupta efficiency [KGE, (Gupta et al., 2009)] (Equation 3) and benchmark efficiency [BE, (Schaefli and Gupta, 2007)] (Equation 4).

$$\mathrm{BIAS} = \frac{\sum_{i=1}^{n}\left(Y_i^{sim} - Y_i^{obs}\right)}{\sum_{i=1}^{n} Y_i^{obs}} X100 \tag{1}$$

$$NSE = 1 - \frac{\sum_{i=1}^{n}\left(Y_i^{obs} - Y_i^{sim}\right)^2}{\sum_{i=1}^{n}\left(Y_i^{obs} - Y_i^{mean}\right)^2} \tag{2}$$

$$\mathrm{KGE} = 1 - \sqrt{(r-1)^2 + \left(\frac{\sigma_{sim}}{\sigma_{obs}} - 1\right)^2 + \left(\frac{\mu_{sim}}{\mu_{obs}} - 1\right)^2} \tag{3}$$

$$\mathrm{BE} = 1 - \frac{\sum_{t=1}^{N}\left[q_{obs}(t) - q_{sim}(t)\right]^2}{\sum_{t=1}^{N}\left[q_{obs}(t) - q_b(t)\right]^2} \tag{4}$$

Y_i^{obs} is data from the observation, Y_i^{sim} data from from the simulation (WRF-Hydro). About the KGE score, r represents the linear correlation between observations and simulations, σ_{obs} is the standard deviation of observations, σ_{sim} is the standard deviation of simulations. μ_{sim} is the mean of simulations and μ_{obs} is the mean of

TABLE 2 Calibration of WRF-Hydro coupled over Senegal River basin.

	SLOPE	REFKDT	MannN	PBL	KGE	NSE	BIAS	BE
Default	0.1	3	Default	5	0.11	−1.17	−18%	−1.30
				7	0.37	−0.18	−41%	−0.25
Overbankflow	0.1	3	Default	5	0.23	0.34	−56%	0.30
Overbankflow	0.08	3	Default	5	0.31	0.41	−51%	0.37
Overbankflow	0.06	3	Default	5	0.49	0.59	−39%	0.57
Overbankflow	0.04	3	Default	5	0.71	0.70	−22%	0.68
				7	0.48	0.60	−41%	0.58
Overbankflow	0.03	3	Default	5	0.83	0.70	−7%	0.67
				7	0.58	0.67	−33%	0.65
Overbankflow	0.01	3	Default	5	0.29	0.17	38%	0.13

observations. q_{obs}, q_{sim} are discharge from observation and simulation data and $q_b(t)$ is the benchmark model discharge at time step t. this benchmark efficiency measures whether the hydrologic model explains more of the observed variability than what is already contained in the seasonality of the climate according Schaefli and Gupta (2007).

To assess the potential impacts of land use change on flooding in the Senegal River basin, an afforestation experiment is conducted using WRF-Hydro model. The calibration performed in Section 2.3 is utilized for our land use change simulations.

The default MODIS land cover map from 2002 (Friedl et al., 2002), considered as a reference, is modified. The principle is to replace savannah with woody savannas found in the upper basin of the river (Figure 2), because this region receives the largest precipitation in the Senegal basin, so a landuse change there can be expected to have the largest hydrological impact. A 10-year simulation is conducted for each of the two scenarios (reference and woody savannas) before evaluating the variation in hydrological components and flooding events.

To assess the model uncertainty of our results, we conduct two 10-year simulations for each of the two planetary boundary layer schemes, PBL5 and PBL7.

The results of these afforestation experiments aim to provide further information on the variation of flooding due to changes in land use in the upper basin of the Senegal River.

3 Results and discussion

3.1 Evaluation of WRF-Hydro precipitation

Figure 3 clearly illustrates that the WRF-Hydro model adequately captures the seasonal fluctuations of precipitation in the Senegal River basin over the period from 2011 to 2020, highlighting a pronounced peak in August for the precipitation.

During the period from January to July, the model appears to reproduce the observed precipitation levels reliably. However, significant divergences emerge between the observed data and the simulations, notably an overestimation in August, followed by an underestimation between September and December. These disparities between observations and modeled results could be attributed to several factors, largely stemming from uncertainties in the input data and in the choice of model physics. This is confirmed who showed that the considerable precipitation variability in West Africa stems from substantial uncertainty in WRF simulations.

3.2 Calibrated discharge

Table 2 shows that WRF-Hydro provides reasonable calibration results (NSE = 0.70; KGE = 0.83; BIAS = −7% and BE = 0.67) and validation results (Figure 5) (NSE = 0.74; KGE = 0.84; BIAS = −8% and BE = 0.73) over the Senegal river basin with the following sensitive parameters SLOPE = 0.03, REFKDF = 3 and default MannN. Similar values of NSE have been found in Benin by Quenum et al. (2022), while focusing in the Oueme river basin (NSE = 0.68). In comparison to other watersheds in the world it is noted that an NSE of 0.30 remains relatively weak but falls within the range of discharge performances published with WRF-Hydro (e.g., Arnault et al., 2016; Kerandi et al., 2018; Rummler et al., 2019; Zhang et al., 2019; Camera et al., 2020; Fersch et al., 2020; Li et al., 2020).

The shift in the discharge curve between the observation and the simulation obtained during our calibration can be partly explained by the quality of the simulated precipitation from the WRF atmospheric model (Figure 4). This is highlighted by Senatore et al. (2015) that the simulated discharge performance with WRF-Hydro is inherently limited by the quality of the simulated precipitation, which constitutes a drawback of the atmospheric-hydrological coupled modeling approach.

3.3 Land cover change experiments

This section is dedicated to the results obtained from modeling land use changes in the upper basin of the Senegal River. The analysis focuses on the changes observed between the reference and the woody savannas scenarios regarding hydrological components and flooding in the Senegal River basin. The principle of land use change modeling is described in Section 2.3 (Figure 2).

3.3.1 Water balance components analysis

Figure 6 illustrates the spatial variation of the main hydrological components obtained through changes between the

reference scenario and the woody savannas scenarios in the upper basin of the Senegal River. The results show an increase in these components, namely evapotranspiration, precipitation, runoff, and percolation, in the area where the replacement (savanna to woody savannas) has been made. These findings regarding the increase in evapotranspiration are similar to those of Camara et al. (2022) conducted in West Africa, where they emphasize that the difference between reforestation and the reference scenario shows an increase in evapotranspiration north of 10° N, with a strong value over the reforested area.

Table 3 shows that the increase can reach around 2% for precipitation (ΔP) 2% for the percolation (ΔRG) and 4% for runoff (ΔRS) with the planetary boundary layer PBL5 in the upper basin of the Senegal River. With PBL7, a drier planetary boundary layer compared to PBL5, an increase of 3% for the precipitation, 5% for the percolation and 7% of runoff is observed in the upper basin. This observed increase in resources is similar to that found in tropical Africa, in the Nzoia basin, East Africa, by Arnault et al. (2023).

As mentioned by Dyn et al. (2014), the increase in rainy days and seasonal precipitation accumulation can be triggered by a change in jet stream structure and an increase in evapotranspiration rate. Our result confirms the importance of the high evapotranspiration rates in the upper parts of the Senegal River basin, where the afforestation experiment is conducted, to modulate precipitation in the region.

3.3.2 Flood events analysis

Figure 7 represents the evolution of floods from 2011 to 2020, characterized by the number of occurrences within a flow of $500m^3/s$. The results show a similar trend between the reference and woody-savannas scenarios, with a high number of occurrences ranging from 500 to 1500 m3/s, followed by a moderately high number of occurrences between 2000 and 3500 m^3/s, and finally a low number of occurrences between 4000 and 6000 m^3/s. Between the two scenarios (reference and woody-savannas), the evolution of occurrences is much more pronounced with pbl5 compared to pbl7, where a significant moderate increase is observed with a peak flow at $4000–4500m^3/s$. The woody-savannas scenario shows the emergence of a peak flow at 5500–6000 m^3/s with pbl5, indicating that the replacement of savannas with woody-savannas scenario potentially results in high flow in the upper basin, which could lead to flooding in the Senegal River basin. This result is consistent with that of (Abiodun et al., 2013) for the coastal region of Nigeria. They mention that afforestation is expected to lead to an increase in the frequency of extreme precipitation events (floods).

The analysis in Figure 8 reveals significant variations in the number of flood occurrences between the reference and woody-savanna scenarios, particularly in the high flow range of 3500 to 6500

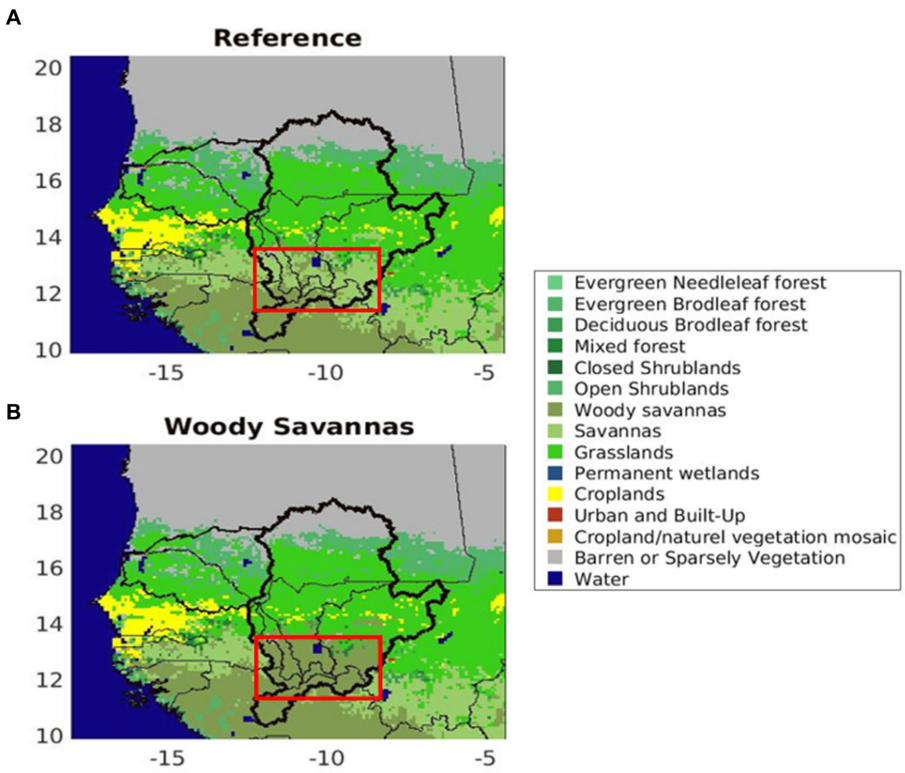

FIGURE 2
Maps of land cover distribution in the Senegal River basin following the MODIS classification (2002) as used in panel **(A)** the reference WRF-Hydro simulation and **(B)** the woody-savannas WRF-Hydro simulation. The black contour line in all the panels indicates the location of the upper basin where the land cover change experiment is conducted. The color classification of MODIS land cover classes is provided in the upper basin side of the figure. The red rectangle represents the area where the change in vegetation cover occurs.

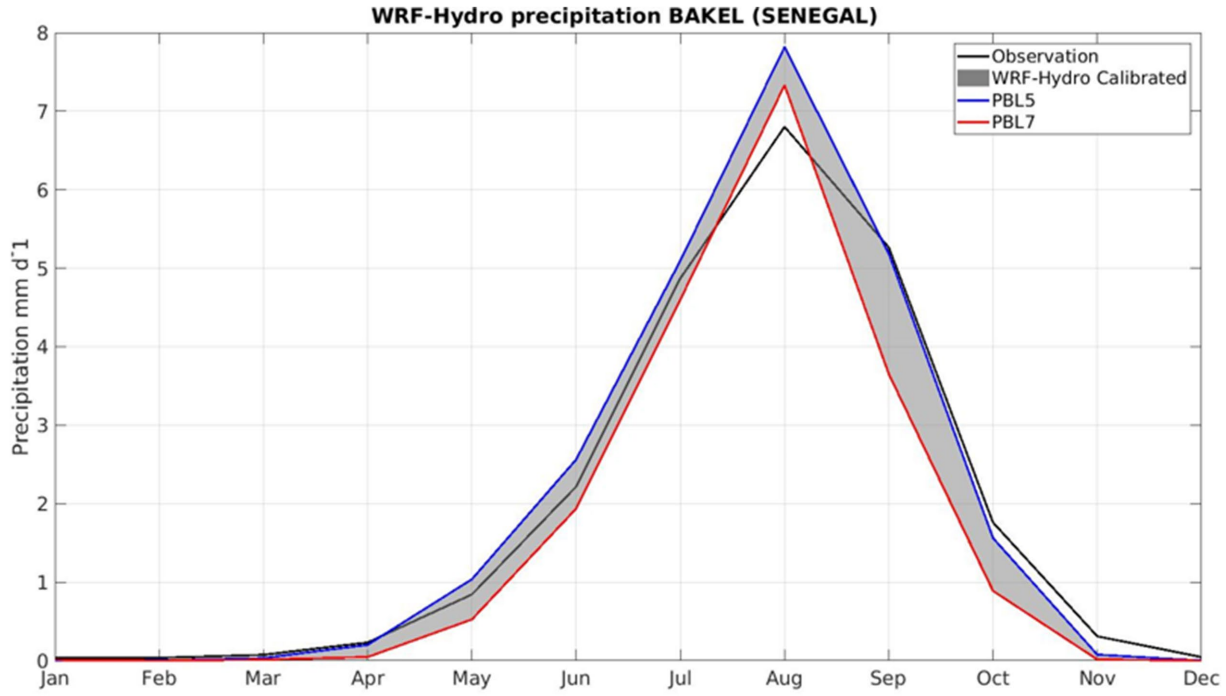

FIGURE 3
Monthly variation of precipitation in the upper basin of the Senegal River. The black curve represents observations from IMERG satellite data. The gray shaded area represents the results of the simulated WRF-Hydro model with the two planetary boundary layers, PBL5 and PBL7.

m3/s. For the planetary boundary layer PBL5, an interesting trend is observed: an increase in the number of occurrences of moderate floods between 3500 and 4000m^3 / s, followed by a decrease in severe floods between 4000 and 5000m^3 / s, and finally, in the emergence of extreme floods above 5000m^3 / s. This observation suggests a complex dynamic of floods in this flow range, with a transition between different levels of flood severity.

Similarly, for the planetary boundary layer PBL7, a positive variation in the number of occurrences is noted, with a peak at 3500–4000m^3 / s. This indicates a distinct response of this scenario to specific flows, potentially highlighting differences in hydrological and meteorological processes between the two scenarios.

These results underline the importance of considering variations in the planetary boundary layer in flood risk analysis with the atmospheric-hydrological modeling approach, in order to account for the uncertainty in the frequency and intensity of extreme events. Furthermore, these results highlight the need for adaptive management of flood-prone areas, considering climate change predictions and evolving environmental conditions.

4 Summary and conclusion

This study aimed to assess the impact of land cover change on floods in the Senegal River basin. To achieve this, the coupled WRF-Hydro model was calibrated and validated for the Senegal River basin. The default 2002 MODIS land cover map, considered as a reference scenario, was modified by replacing savannas with woody savannas in the river's upper basin. Subsequently, a 10-year simulation was conducted with calibrated WRF-Hydro for each scenario (reference scenario and woody-savannas scenario). An evaluation of the hydrological components and flood events was performed between the two scenarios (woody-savannas - reference).

Our results show that afforestation increases precipitation, actual evapotranspiration and runoff in the area where savanna was converted to woody savannas. This increase in water resources amounts to approximately +2% in precipitation and + 4% in runoff in the upper basin of the river. With the planetary PBL5, a significant increase in the number of flood occurrences is observed in the Senegal River basin. Specifically, there is an increase of 17 occurrences in moderate floods between 3000 and 4000 m^3/s, followed by a slight decrease of 2 occurrences in severe floods between 4000 and 5000 m^3/s. Finally, there is an increase of around 2 occurrences in extreme floods above 5000 m^3/s. In summary, replacing savanna with woody-savannas (woody-savannas) in the upper basin of the Senegal River has the potential to increase water resources upstream of Bakel but also lead to more extreme flooding downstream. This study highlights the complex interaction between land use change, water resources, and flood dynamics. It emphasizes the importance of holistic approaches to land management that consider both local and downstream impacts, thereby contributing valuable insights for sustainable development and risk reduction strategies in the Senegal River basin and similar regions. However, it is essential to consider several sources of uncertainties in this analysis. First, the afforestation strategy followed can significantly influence the results. The choice of tree species, planting density, and the precise location of the reforested areas can all have varying impacts on hydrological processes and surface flows.

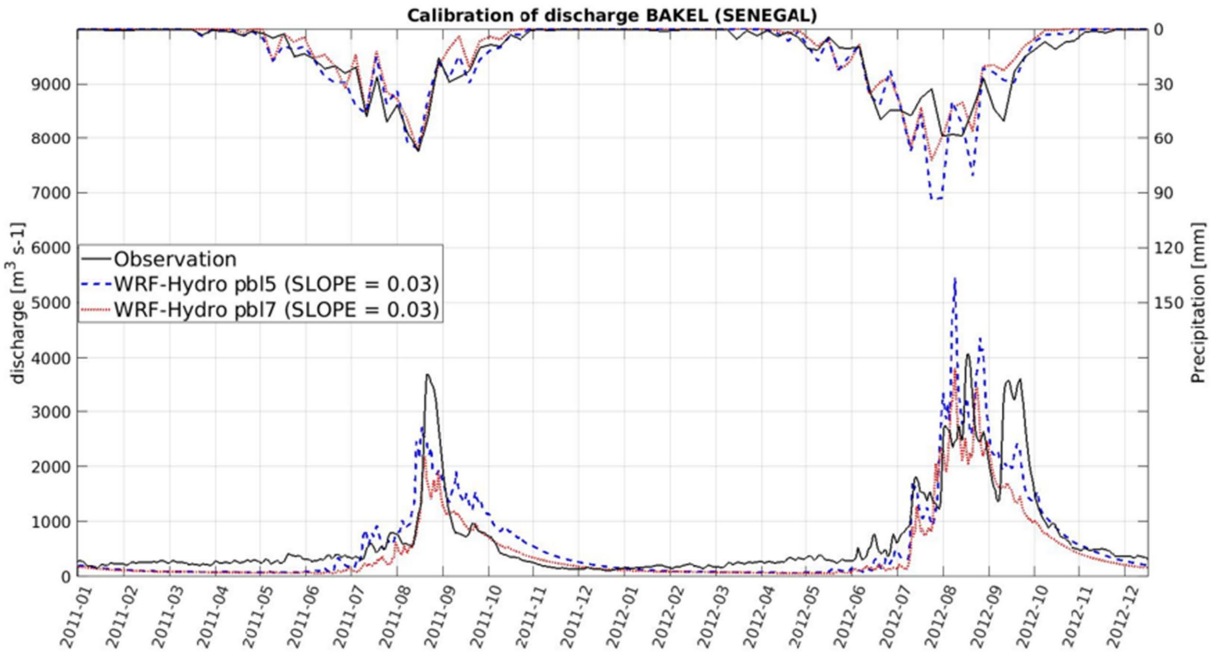

FIGURE 4
Calibration of discharge: at the bottom, daily time series of discharge Q (in m^3/s) for a two-year period from 1st January 2011 to 31st December 2012 derived from the observational product BAKEL station outlet of the upper basin (in black); and discharge from calibrated WRF-Hydro simulations with PBL5 (in blue) and PBL7 (in red). At the top, weekly accumulation of precipitation from IMERG satellite data (in black) and precipitation from calibrated WRF-Hydro simulations with PBL5 (in blue) and PBL7 (in red).

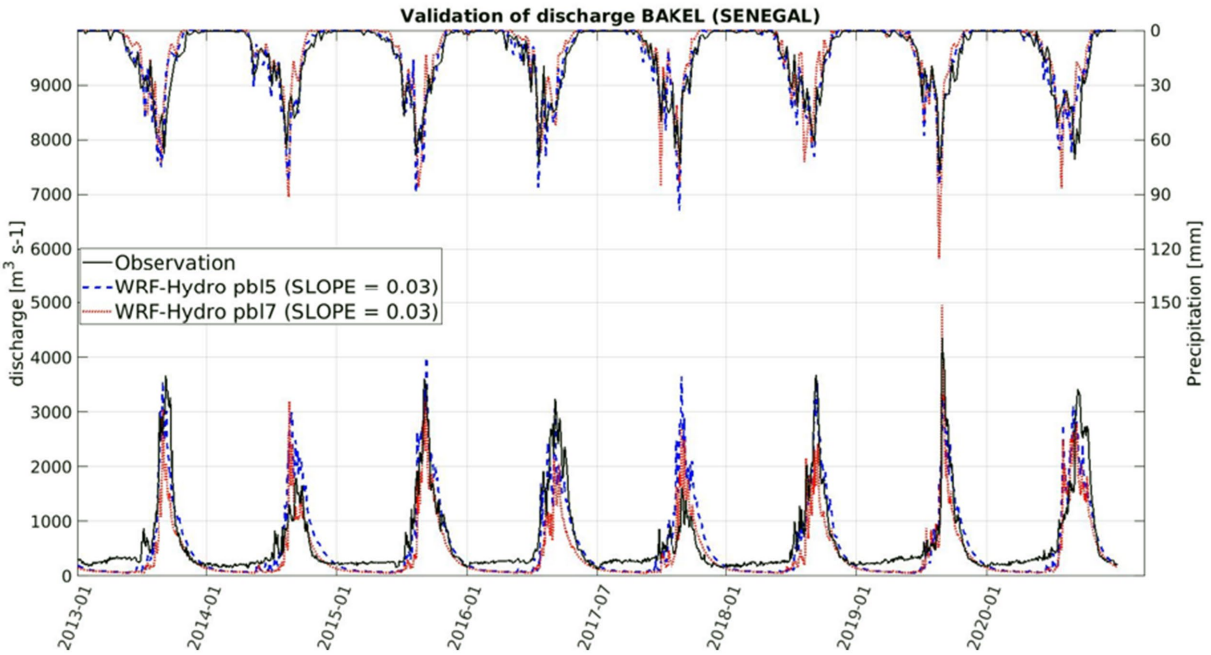

FIGURE 5
Validation of discharge: at the bottom, daily time series of discharge Q (in m^3/s) for a two-year period from 1st January 2013 to 31st December 2020 derived from the observational product BAKEL station outlet of the upper basin (in black); and discharge from calibrated WRF-Hydro simulations with PBL5 (in blue) and PBL7 (in red). At the top, weekly accumulation of precipitation from IMERG satellite data (in black) and precipitation from calibrated WRF-Hydro simulations with PBL5 (in blue) and PBL7 (in red).

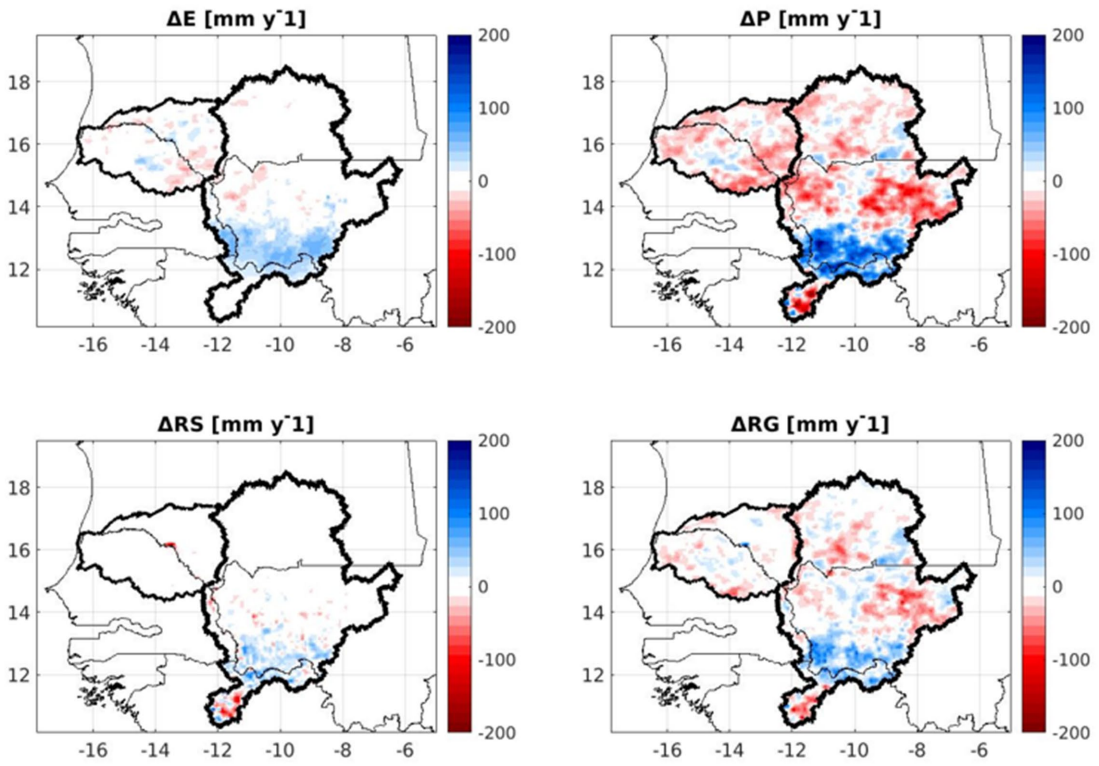

FIGURE 6
Spatial variation of the mean (PBL5 and PBL7) of water balance components Precipitation, Evapotranspiration, Surface Runoff and Sub-surface Runoff calculated with Woody-savannas – Reference scenarios. The dark curve represents Senegal River basin.

TABLE 3 Mean annual change over all the upper basin.

Boundary planetary layers	ΔP Annual precipitation change	ΔRG Annual percolation change	ΔRS Annual Runoff change	ΔE Annual Evapotranspiration change
PBL5	+2%	+2%	+4%	+2
PBL7	+3%	+5%	+7%	+1

Our results are consistent with those of Abiodun et al. (2013), which show that afforestation induces a more frequent occurrence of extreme rainfall events (flooding) in the coastal region of Nigeria.

To go further, it would be useful to determine the ability of the WRF-Hydro model to forecast floods in the Senegal River basin and to develop a hypothesis on changes in vegetation cover to identify ways to reduce flooding in the lower part of the basin.

These findings have significant implications for policymakers and planners involved in land cover management, water resource management, and disaster risk reduction. They underscore the importance of considering not only the immediate benefits of afforestation but also its potential downstream consequences, particularly in flood-prone areas.

Data availability statement

The original contributions presented in the study are included in the article/supplementary material, further inquiries can be directed to the corresponding author.

Author contributions

AN: Conceptualization, Data curation, Formal analysis, Investigation, Methodology, Software, Visualization, Writing – original draft, Writing – review & editing. JA: Conceptualization, Formal analysis, Investigation, Methodology, Software, Supervision, Validation, Visualization, Writing – review & editing. MM: Data curation, Supervision, Validation, Visualization, Writing – review & editing. SS: Supervision, Validation, Visualization, Writing – review & editing. MC: Supervision, Validation, Visualization, Writing – review & editing. AL: Supervision, Validation, Visualization, Writing – review & editing. HK: Supervision, Validation, Visualization, Writing – review & editing.

Funding

The author(s) declare that financial support was received for the research, authorship, and/or publication of this article. This paper is part of a doctoral research initiative, generously funded by the

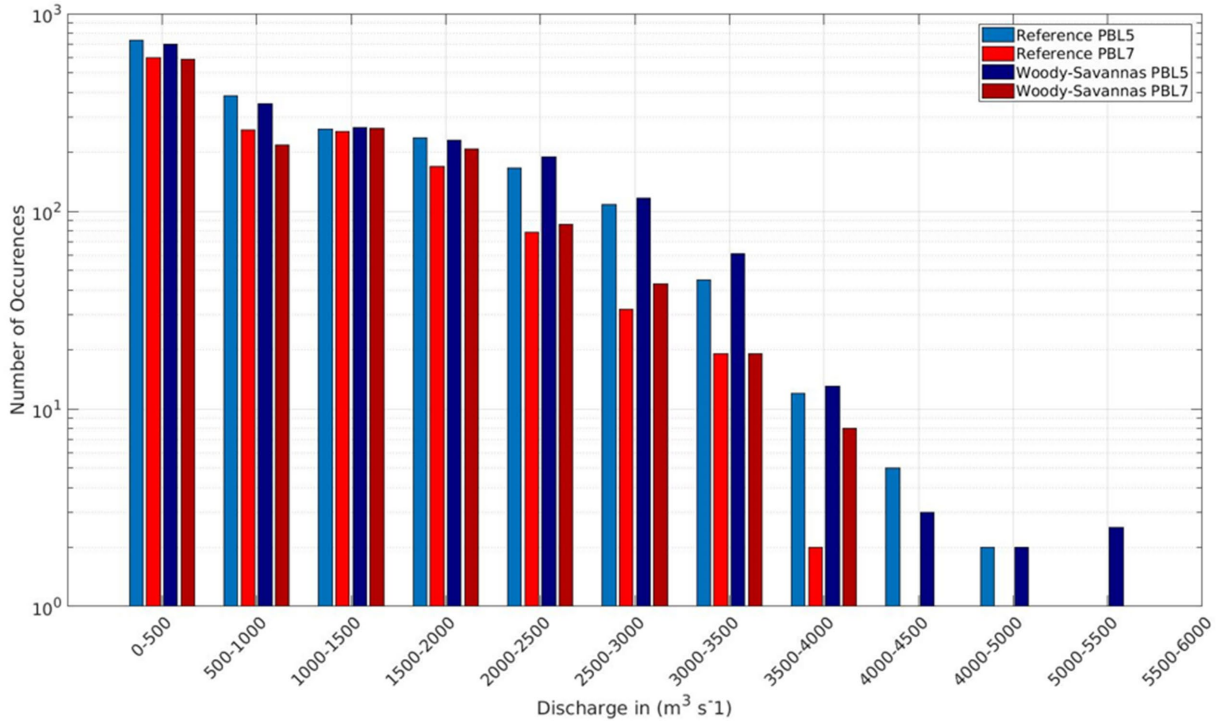

FIGURE 7
Variation in occurrence numbers based on the flow rate bins covering a 500 m^3s^{-1} range. The red color represents the Reference scenario (PBL5 and PBL7), while the blue color represents the Woody-savannas scenario (PBL5 and PBL7).

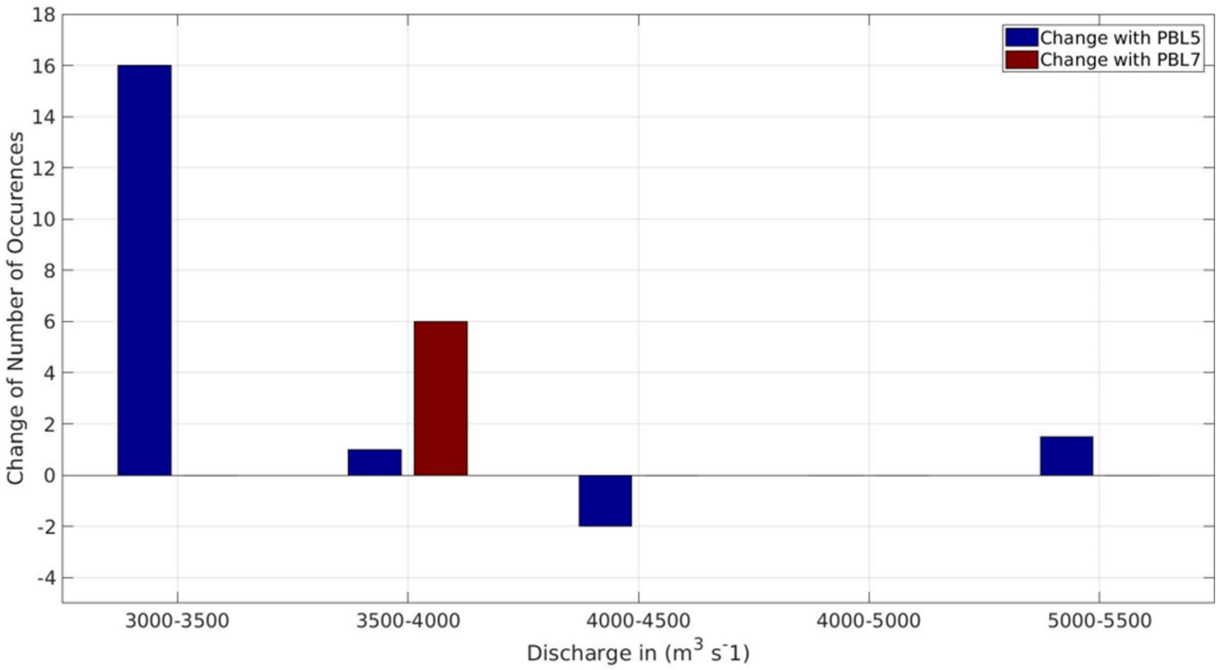

FIGURE 8
Change in occurrence numbers based on the high flow rate range (3500 to 5500 m^3/s) between Reference scenario and Woody-savannas scenario. The blue color represents the mean change between the Reference and Woody-savannas scenarios with the planetary boundary layer PBL5. The red color represents the mean change between the Reference and Woody-savannas scenarios with the planetary boundary layer PBL7.

German Federal Ministry of Education and Research (BMBF) through the West Africa Science Center of Climate Change and Adapted Land Use (WASCAL).

Acknowledgments

The simulations were conducted on the Linux cluster at KIT/IMK-IFU in Garmisch-Partenkirchen. Special thanks to the Federal Ministry of Education and Research of Germany (BMBF) through the West African Science Service Center on Climate Change and Adapted Land Use (WASCAL), and the German Science Foundation (DFG) through the Large-Scale and High-Resolution Mapping of Soil Moisture on Field and Catchment Scales Boosted by Cosmic-Ray Neutrons (COSMIC-SENSE, FOR 2694, grant KU 2090/12-2). Thanks to the project team of CONCERT (*Greenhouse gas emissions and mitigation options under climate and land use change in West Africa: A concerted regional modeling and observation assessment*). Thanks to the Concerted Regional Modeling and Observation Assessment for Greenhouse Gas Emissions and Mitigation Options under Climate and Land Use Change in West Africa (CONCERT-West Africa project; grant number 01LG2089A BMBF) for supporting this research. Thanks also to the Directorate of Water Resources Management and Planning of Senegal (DGPRE) for providing the river flow data.

Conflict of interest

The authors declare that the research was conducted in the absence of any commercial or financial relationships that could be construed as a potential conflict of interest.

Publisher's note

All claims expressed in this article are solely those of the authors and do not necessarily represent those of their affiliated organizations, or those of the publisher, the editors and the reviewers. Any product that may be evaluated in this article, or claim that may be made by its manufacturer, is not guaranteed or endorsed by the publisher.

References

Abiodun, B. J., Salami, A. T., Matthew, O. J., and Odedokun, S. (2013). Potential impacts of afforestation on climate change and extreme events in Nigeria. *Clim. Dyn.* 41, 277–293. doi: 10.1007/s00382-012-1523-9

Acuña-Alonso, C., Novo, A., Rodríguez, J. L., Varandas, S., and Álvarez, X. (2022). Modelling and evaluation of land use changes through satellite images in a multifunctional catchment: social, economic and environmental implications. *Eco. Inform.* 71:101777. doi: 10.1016/j.ecoinf.2022.101777

Arnault, J., Mwanthi, A. M., Portele, T., Li, L., Rummler, T., Fersch, B., et al. (2023). Regional water cycle sensitivity to afforestation: synthetic numerical experiments for tropical Africa. *Front. Clim.* 5:1233536. doi: 10.3389/fclim.2023.1233536

Arnault, J., Wagner, S., Rummler, T., Fersch, B., Bliefernicht, J., Andresen, S., et al. (2016). Role of runoff-infiltration partitioning and resolved overland flow on land-atmosphere feedbacks: a case study with the WRF-hydro coupled modeling system for West Africa. *J. Hydrometeorol.* 17, 1489–1516. doi: 10.1175/JHM-D-15-0089.1

Astou Sambou, M. H., Albergel, J., Vissin, E. W., Liersch, S., Koch, H., Szantoi, Z., et al (2023). Prediction of land use and land cover change in two watersheds in the Senegal River basin (West Africa) using the Multilayer Perceptron and Markov chain model. *European Journal of Remote Sensing*, 56. doi: 10.1080/22797254.2023.2231137

Babaei, S., Ghazavi, R., and Erfanian, M. (2018). Urban flood simulation and prioritization of critical urban sub-catchments using SWMM model and PROMETHEE II approach. *Phys. Chem. Earth* 105, 3–11. doi: 10.1016/j.pce.2018.02.002

Banjara, M., Bhusal, A., Ghimire, A. B., and Kalra, A. (2024). Impact of land use and land cover change on hydrological processes in urban watersheds: Analysis and Forecasting for Flood Risk Management. Geosciences (Switzerland). *Geosciences* 14:40. doi: 10.3390/geosciences14020040

Camara, M., Diba, I., and Diedhiou, A. (2022). Effects of land cover changes on compound extremes over West Africa using the regional climate model Reg CM4. *Atmosphere* 13:17. doi: 10.3390/atmos13030421

Camera, C., Bruggeman, A., Zittis, G., Sofokleous, I., and Arnault, J. (2020). Simulation of extreme rainfall and streamflow events in small Mediterranean watersheds with a one-way-coupled atmospheric-hydrologic modelling system. *Nat. Hazards Earth Syst. Sci.* 20, 2791–2810. doi: 10.5194/nhess-20-2791-2020

Cardona, O. D., Van Aalst, M. K., Birkmann, J., Fordham, M., Mc Gregor, G., Rosa, P., et al. (2012). Determinants of risk: Exposure and vulnerability. *Managing the Risks of Extreme Events and Disasters to Advance Climate Change Adaptation: Special Report of the Intergovernmental Panel on Climate Change*, 9781107025, 65–108. doi: 10.1017/CBO9781139177245.005

Costache, R., Hong, H., and Wang, Y. (2019). Identification of torrential valleys using GIS and a novel hybrid integration of artificial intelligence, machine learning and bivariate statistics. *Catena* 183:104179. doi: 10.1016/j.catena.2019.104179

Déqué, M., Calmanti, S., Christensen, O. B., Dell Aquila, A., Maule, C. F., Haensler, A., et al. (2017). A multi-model climate response over tropical Africa at +2 °C. *Clim. Ser.* 7, 87–95. doi: 10.1016/j.cliser.2016.06.002

Dudhia, J. (1989). Numerical study of convection observed during the winter monsoon experiment using a mesoscale two-dimensional model. *J. Atmos. Sci.* 46, 3077–3107. doi: 10.1175/1520-0469(1989)046<3077:NSOCOD>2.0.CO;2

Dyn, C., Hagos, S., Leung, L. R., and Xue, Y. (2014). Assessment of uncertainties in the response of the African monsoon precipitation to land use change simulated by a regional model. *Clim. Dynamics* 43:1975. doi: 10.1007/s00382-014-2092-x

Faty, A., Kouame, F., Niang Fall, A., and Kane, A. (2019). Land use dynamics in the context of variations in hydrological regimes in the upper Senegal River basin. *Int. J. Hydrol.* 3, 185–192. doi: 10.15406/ijh.2019.03.00179

Faye, C., Sow, A. A., and Ndong, J. B. (2015). Étude des sècheresses pluviométriques et hydrologiques en Afrique tropicale: caractérisation et cartographie de la sècheresse par indices dans le haut bassin du fleuve Sénégal. *Physio-Géo* 9, 17–35. doi: 10.4000/physio-geo.4388

Fersch, B., Senatore, A., Adler, B., Arnault, J., Mauder, M., Schneider, K., et al. (2020). High-resolution fully coupled atmospheric-hydrological modeling: a cross-compartment regional water and energy cycle evaluation. *Hydrol. Earth Syst. Sci.* 24, 2457–2481. doi: 10.5194/hess-24-2457-2020

Fofana, M., Adounkpe, J., Larbi, I., Hounkpe, J., Djan'na Koubodana, H., Toure, A., et al. (2022). Urban flash flood and extreme rainfall events trend analysis in Bamako, Mali. *Environ. Challeng.* 6, 100449–100448. doi: 10.1016/j.envc.2022.100449

Friedl, M. A., McIver, D. K., Hodges, J. C. F., Zhang, X. Y., Muchoney, D., Strahler, A. H., et al. (2002). Global land cover mapping from MODIS: algorithms and early results. *Remote Sens. Environ.* 83, 287–302. doi: 10.1016/S0034-4257(02)00078-0

Gochis, D. J., Barlage, M., Cabell, R., Casali, M., Dugger, A., FitzGerald, K, et al. (2021). The NCAR WRF-hydro modeling system technical description. User Manual, Version 5.1.1., 108. Available at:https://ral.ucar.edu/sites/default/files/public/WRFHydroV511TechnicalDescription.pdf.

Gochis, D. J., Barlage, M., Cabell, R., Casali, M., Dugger, A., Fitzgerald, K., et al., (2020). The NCAR WRF-hydro® modeling system technical description until further notice, please cite the WRF-hydro® modeling system as follows. Available at:https://ral.ucar.edu/sites/default/files/public/WRFHydroV511TechnicalDescription.pdf.

Grell, G. A., and Freitas, S. R. (2014). A scale and aerosol aware stochastic convective parameterization for weather and air quality modeling. *Atmos. Chem. Phys.* 14, 5233–5250. doi: 10.5194/acp-14-5233-2014

Gupta, H. V., Kling, H., Yilmaz, K. K., and Martinez, G. F. (2009). Decomposition of the mean squared error and NSE performance criteria: implications for improving hydrological modelling. *J. Hydrol.* 377, 80–91. doi: 10.1016/j.jhydrol.2009.08.003

Hall, J., Arheimer, B., Borga, M., Brázdil, R., Claps, P., Kiss, A., et al. (2014). Understanding flood regime changes in Europe: a state-of-the-art assessment. *Hydrol. Earth Syst. Sci.* 18, 2735–2772. doi: 10.5194/hess-18-2735-2014

Hersbach, H., Bell, B., Berrisford, P., Hirahara, S., Horányi, A., Muñoz-Sabater, J., et al. (2020). The ERA5 global reanalysis. *Q. J. R. Meteorol. Soc.* 146, 1999–2049. doi: 10.1002/qj.3803

Hirabayashi, Y., Alifu, H., Yamazaki, D., Imada, Y., Shiogama, H., and Kimura, Y. (2021). Anthropogenic climate change has changed frequency of past flood during 2010-2013. *Prog Earth Planet Sci*. 8:9. doi: 10.1186/s40645-021-00431-w

Hong, S., and Lim, J. (2006). The WRF single-moment 6-class microphysics scheme (WSM6). *Journal of the Korean Meteorological Society*. 42, 129–151.

Huffman, G. J., Bolvin, D. T., Braithwaite, D., Hsu, K., Joyce, R., and Xie, P. (2014). NASA global precipitation measurement (GPM) integrated multi-satellitE retrievals for GPM (IMERG). Algorithm theoretical basis document (ATBD) version 4.4. National Aeronautics and Space Administration (NASA), February, 1–31. Available at: https://gpm.nasa.gov/sites/default/files/document_files/IMERG_ATBD_V5.2_0.pdf%0Ahttps://pmm.nasa.gov/sites/default/files/document_files/IMERG_ATBD_%0AV4.4.pdf

Kadri, T., and Kurniyaningrum, E. (2019). Impact of land use on frequency of floods in upper Bekasi watershed, Indonesia. *Int. J. Sci. Technol. Res.* 8, 3328–3334.

Kerandi, N., Arnault, J., Laux, P., Wagner, S., Kitheka, J., and Kunstmann, H. (2018). Joint atmospheric-terrestrial water balances for East Africa: a WRF-hydro case study for the upper Tana River basin. *Theor. Appl. Climatol.* 131, 1337–1355. doi: 10.1007/s00704-017-2050-8

Konate, D., Didi, S. R., Dje, K. B., Diedhiou, A., Kouassi, K. L., Kamagate, B., et al. (2023). Observed changes in rainfall and characteristics of extreme events in C ô te d' Ivoire (West Africa). *Hydrology* 10:104. doi: 10.3390/hydrology10050104

Kundzewicz, Z. W., Kanae, S., Seneviratne, S. I., Handmer, J., Nicholls, N., Peduzzi, P., et al. (2014). Le risque d'inondation et les perspectives de changement climatique mondial et régional. *Hydrol. Sci. J.* 59, 1–28. doi: 10.1080/02626667.2013.857411

Lehner, B., Verdin, K., and Jarvis, A. (2008). New global hydrography derived from spaceborne elevation data. *Eos* 89, 93–94. doi: 10.1029/2008EO100001

Li, L., Pontoppidan, M., Sobolowski, S., and Senatore, A. (2020). The impact of initial conditions on convection-permitting simulations of a flood event over complex mountainous terrain. *Hydrol. Earth Syst. Sci.* 24, 771–791. doi: 10.5194/hess-24-771-2020

Mlawer, E. J., Taubman, S. J., Brown, P. D., Iacono, M. J., and Clough, S. A. (1997). Radiative transfer for inhomogeneous atmospheres: RRTM, a validated correlated-k model for the longwave. *J. Geophys. Res. Atmos.* 102, 16663–16682. doi: 10.1029/97jd00237

Mmom, P. C., and Aifesehi, P. E. E. (2013). Vulnerability and resilience of Niger Delta coastal communities to flooding. *IOSR J. Human. Soc. Sci.* 10, 27–33. doi: 10.9790/0837-1062733

Najibi, N., and Devineni, N. (2018). Recent trends in the frequency and duration of global floods. *Earth Syst. Dynam.* 9, 757–783. doi: 10.5194/esd-9-757-2018

Nakanishi, M., and Niino, H. (2004). An improved Mellor–Yamada level-3 model with condensation physics: Its design and verification. *Bound.-Layer Meteorol*, 112:1–31. doi: 10.1023/B:BOUN.0000020164.04146.98

Nash, J. E., and Sutcliffe, J. V. (1970). River flow forecasting through conceptual models-part I-A discussion of principles. *J. Hydrol.* 10, 282–290. doi: 10.1016/0022-1694(70)90255-6

Ndiaye, A., Mbaye, M. L., Arnault, J., Camara, M., and Lawin, A. E. (2023). Characterization of extreme rainfall and river discharge over the Senegal River basin from 1982 to 2021. *Hydrology* 10:204. doi: 10.3390/hydrology10100204

Ndiaye, P. M., Bodian, A., Diop, L., Dezetter, A., Guilpart, E., Deme, A., et al. (2021). Future trend and sensitivity analysis of evapotranspiration in the Senegal River basin. *J. Hydrol. Reg. Stud.* 35:100820. doi: 10.1016/j.ejrh.2021.100820

Niu, G. Y., Yang, Z. L., Mitchell, K. E., Chen, F., Ek, M. B., Barlage, M., et al. (2011). The community Noah land surface model with multiparameterization options (Noah-MP): 1. Model description and evaluation with local-scale measurements. *J. Geophys. Res. Atmos.* 116, 1–19. doi: 10.1029/2010JD015139

Pleim, J. E. (2007). A combined local and nonlocal closure model for the atmospheric boundary layer. Part I: model description and testing. *J. Appl. Meteorol. Climatol.* 46, 1383–1395. doi: 10.1175/JAM2539.1

Prăvălie, R., Bandoc, G., Patriche, C., and Sternberg, T. (2019). Recent changes in global drylands: evidences from two major aridity databases. *Catena* 178, 209–231. doi: 10.1016/j.catena.2019.03.016

Quenum, G. M. L. D., Arnault, J., Klutse, N. A. B., Zhang, Z., Kunstmann, H., and Oguntunde, P. G. (2022). Potential of the coupled WRF/WRF-hydro modeling system for flood forecasting in the Ouémé River (West Africa). *Water (Switzerland)* 14:1192. doi: 10.3390/w14081192

Rogger, M., Agnoletti, M., Alaoui, A., Bathurst, J. C., Bodner, G., Borga, M., et al. (2017). Land use change impacts on floods at the catchment scale: challenges and opportunities for future research. *Water Resour. Res.* 53, 5209–5219. doi: 10.1002/2017WR020723

Rummler, T., Arnault, J., Gochis, D., and Kunstmann, H. (2019). Role of lateral terrestrial water flow on the regional water cycle in a complex terrain region: investigation with a fully coupled model system. *J. Geophys. Res. Atmos.* 124, 507–529. doi: 10.1029/2018JD029004

Schaefli, B., and Gupta, H. V. (2007). "Do Nash Values Have Value?, Hydrol. Process." 21, 2075–2080. doi: 10.1002/hyp.6825.2007

Senatore, A., Mendicino, G., Gochis, D. J., Yu, W., Yates, D. N., and Kunstmann, H. (2015). Fully coupled atmosphere-hydrology simulations for the central Mediterranean: Impact of enhanced hydrological parameterization for short and long time scales. *J. Adv. Model. Earth Syst.* 7, 1693–1715. doi: 10.1002/2015MS000510

Skamarock, W. C., Klemp, J. B., Dudhia, J. B., Gill, D. O., Barker, D. M., Duda, M. G., et al. (2021). A Fully Compressible Nonhydrostatic Deep-Atmosphere Equations Solver for MPAS. *Monthly Weather Review*, 149, 571–83.

Stisen, S., Jensen, K. H., Sandholt, I., and Grimes, D. I. F. (2008). A remote sensing driven distributed hydrological model of the Senegal River basin. *J. Hydrol.* 354, 131–148. doi: 10.1016/j.jhydrol.2008.03.006

Sy, S., de Noblet-Ducoudré, N., Quesada, B., Sy, I., Dieye, A. M., Gaye, A. T., et al. (2017). Land-surface characteristics and climate in West Africa: models' biases and impacts of historical anthropogenically-induced deforestation. *Sustainability* 9, 1–24. doi: 10.3390/su9101917

Sy, S., and Quesada, B. (2020). Anthropogenic land cover change impact on climate extremes during the 21st century. *Environ. Res. Lett.* 15:9. doi: 10.1088/1748-9326/ab702c

Ta, S., Kouadio, K. Y., Ali, K. E., Toualy, E., Aman, A., and Yoroba, F. (2016). West Africa extreme rainfall events and large-Scale Ocean surface and atmospheric conditions in the tropical Atlantic. *Adv. Meteorol.* 2016, 1–14. doi: 10.1155/2016/1940456

Tazen, F., Diarra, A., Kabore, R. F. W., Ibrahim, B., Bologo\/Traoré, M., Traoré, K., et al. (2019). Trends in flood events and their relationship to extreme rainfall in an urban area of Sahelian West Africa: the case study of Ouagadougou, Burkina Faso. *J. Flood Risk Manage.* 12:12. doi: 10.1111/jfr3.12507

Thapa, N., and Prasai, R. (2022). Impacts of floods in land use land cover change: a case study of Indrawati and Melamchi River, Melamchi and Indrawati municipality, Nepal. *Int. J. Multidiscipl. Res. Growth Evalu.* 3:374–384. doi: 10.54660/anfo.2022.3.5.18

Young, H. R., Cornforth, R. J., Gaye, A. T., and Boyd, E. (2019). Event attribution science in adaptation decision-making: the context of extreme rainfall in urban Senegal. *Clim. Dev.* 11, 812–824. doi: 10.1080/17565529.2019.1571401

Zermoglio, F., Steynor, A., and Jack, C. (2015). Climate change and health risks in Senegal.

Zhang, Z., Arnault, J., Wagner, S., Laux, P., and Kunstmann, H. (2019). Impact of lateral terrestrial water flow on land-atmosphere interactions in the Heihe River basin in China: fully coupled modeling and precipitation recycling analysis. *J. Geophys. Res. Atmos.* 124, 8401–8423. doi: 10.1029/2018JD030174